

Computational Fluid Dynamics Analysis and Correlation with Intraoperative Aneurysm Features



Alberto Feletti, Xiangdong Wang, Sandeep Talari, Tushit Mewada, Dilshod Mamadaliev, Riki Tanaka, Yasuhiro Yamada, Yamashiro Kei, Daisuke Suyama, Tukasa Kawase, and Yoko Kato

Abstract *Introduction.* There are many controversies about computational fluid dynamics (CFD) findings and aneurysm initiation, growth, and ultimate rupture. The aim of our work was to analyze CFD data in a consecutive series of patients and to correlate them with intraoperative visual aneurysm findings.

Methods. Hemoscope software (Amin, Ziosoft Corporation, Minato ward, Tokyo, Japan) was used to process images from 17 patients who underwent clipping of 18 aneurysms. Pressure (P), wall shear stress (WSS) gradient and vectors, normalized WSS, and streamlines (SL) direction and velocity were assessed. CFD data were compared to intraoperative visual findings. A total of 39 aneurysm wall areas were assessed.

Results. Red, thin aneurysm wall areas were more often associated with low WSS. However, the association of low WSS with high P , diverging WSS vectors, direct impact of SL, and high SL velocity more frequently matched with yellow, atherosclerotic aneurysm walls.

Conclusions. Low WSS alone is not sufficient to determine the thickness of an aneurysm wall. Its association with other parameters might enable one to distinguish preoperatively atherosclerotic, thick areas (high P , diverging WSS vectors, high flow velocity) from thin areas with higher rupture risk (parallel WSS vectors, lower flow

velocity). The changing balance between these parameters can modify the features and the risk of rupture of aneurysm wall over time.

Keywords Computational fluid dynamics (CFD) · Aneurysm · Wall shear stress (WSS) · Pressure · Streamlines · Intraoperative

Introduction

The possibility to predict the natural history of unruptured intracranial aneurysms (UIAs) would be of the utmost importance for both patient and surgeon. Surgeons could more precisely assess the risk of rupture, therefore advising surgery only for those patients whose rupture risk is higher than the risks of the treatment. Moreover, surgeons could have a clearer preoperative knowledge of not only the shape and the position of the aneurysm, but also the features of its wall. Knowing in advance whether an area of the wall is thinner or thicker could help in the surgical planning, and potentially reduce the risks of intraoperative rupture. This would be even more important before starting coiling an aneurysm. Computational fluid dynamics (CFD) analysis is considered a promising tool in order to understand better aneurysm initiation, growth, and eventual rupture [1, 2]. The majority of studies have so far been focused on prediction of rupture [3–7]. However, the analysis of several CFD hemodynamic factors has led to controversial results [4, 8]. Moreover, only a few published papers have analyzed the correspondence between CFD parameters and the features of the aneurysm wall [1, 9].

With the aim of finding potential correlation between CFD hemodynamic factors and the characteristics of the aneurysm wall, we prospectively applied CFD analysis to a series of 18 UIAs, and compared the results with intraoperative anatomical findings.

A. Feletti, M.D., Ph.D. (✉)

Department of Neurosciences, Neurosurgery Unit, NOCSAE
Modena Hospital, Modena, Italy

Department of Neurosurgery, Fujita Health University Hospital,
Nagoya, Japan

X. Wang, M.D., Ph.D. · S. Talari, M.D. · T. Mewada, M.D.

D. Mamadaliev, M.D. · R. Tanaka, M.D.

Y. Yamada, M.D., Ph.D. · Y. Kei, M.D. · D. Suyama, M.D.

T. Kawase, M.D., Ph.D. · Y. Kato, M.D., Ph.D.

Department of Neurosurgery, Fujita Health University Hospital,
Nagoya, Japan

Materials and Methods

Case Series

Eighteen UIAs clipped in 17 patients during 17 procedures between February and May 2016 have been included in the study. The population included 4 males and 13 females with a mean age of 64 years (range 41–77 years). Aneurysm locations, sizes, and patients' demographics are summarized in Table 1.

The study protocol was approved by the local ethics committee of our institution.

Computational Fluid Dynamics Modeling

Head digital subtraction angiography images were processed via manual cropping and thresholding, and converted into a triangulated surface through Ziosoft (Amin Corp, Minato ward, Tokyo, Japan), obtaining the geometry of blood vessels and aneurysms. An unstructured computational volumetric mesh was built from the triangulated surface. The mesh was composed of tetrahedrons and prism element layers to improve the analytic precision of the boundary layer. Hemoscope software (Amin Corp, Minato ward, Tokyo, Japan) used the Navier–Stokes equations to

simulate blood flow on the computational mesh, assuming pulsatile laminar flow, zero pressure at the blood vessel outlet, Newtonian fluid, and rigid blood vessel walls with non-slip conditions. For each aneurysm we investigated instantaneous maximum pressure (P), instantaneous wall shear stress magnitude (WSSm), cycle variation WSS (cvWSS), wall shear stress vectors (WSSv), and streamlines velocity and direction (SL). WSS and velocity were also normalized by parent vessel values generated from the same CFD simulation to minimize the dependence on inlet conditions.

Operative Procedure

All patients have been operated on using a ZeissFlow 800 OPMI Pentero surgical microscope (Zeiss, Oberkochen, Germany) with motor evoked potential (MEP) monitoring in selected cases. Pre-clipping and post-clipping ICG-VA were performed in all cases. A rigid endoscope (Machida, Japan) was always used to inspect eventual perforators and to have a better vision of the walls of the aneurysm that were not visible by the microscope. All operations have been video-recorded. For every aneurysm, we checked for the presence of eventual areas characterized by either red, translucent walls or white-yellow, atherosclerotic walls during surgery. As in previous studies, the surfaces with red color and translucence were defined as thin-walled (TW), compared with healthy areas of parent vessels. The surfaces with yellow-white color and opaqueness were defined as thick-walled and atherosclerotic (AW). A total of 39 areas have been identified, directly visually inspected, and compared with CFD data.

Table 1 Aneurysm data and patients' demographics

Patient	Sex, age	Aneurysm location	Aneurysm size (mm)
1	F, 57	Lt ICA bif	4
2	F, 65	Lt MCA M1	6
3	F, 77	Rt MCA M2	9
4	M, 41	Lt VA	10
5	F, 60	Lt ICA	6
6	F, 64	Acom	12
7	F, 73	Rt MCA	3
8	M, 76	Lt MCA	4
9	F, 71	Lt ICPC	6
10	F, 73	A2-A3	6
11	M, 57	Acom	8
12	F, 67	Lt MCA prox	4
		Lt MCA dist	3
13	F, 52	Rt ICA C2	8
14	F, 63	Lt MCA bif	5
15	F, 65	Acom	4
16	F, 70	Rt MCA	5
17	M, 62	Lt ICPC	8

Statistical Analysis

Continuous data are shown as mean \pm SD. We used the t test for the comparison of mean values. An overall significance level of $p < 0.05$ was adopted.

Results

Among 39 microsurgically-visualized areas, we identified 12 TW areas and 19 AW areas in 18 aneurysms (Table 2). We found that the association of high P , low WSS, divergent WSS vectors, and streamlines hitting the wall with high velocity is more often associated with AW areas (78.6% of cases; Fig. 1). In these cases, the mean normalized WSS was

Table 2 CFD data and intraoperative findings

Patient	Aneurysm	Area	nP	nWSS	nVel	hP, IWSS, dWSSv, hitSL	WSS	Intraop
1	Lt ICA bif	1	99.7	5	38.1		Low	TW
		2	99.8	1	90.48	Yes	Low	AW
		3	99.7	5	19.05		Low	AW
2	LtMCA	4	100	0.32	100	Yes	Low	AW
		5	99.9	0.32	40	Yes	Low	AW
		6	99.8	0.32	16.67		Low	AW
		7	99.8	96.77	83.33		High	Normal
3	Rt MCA	8	99.8	0.54	8		Low	TW
		9	99.8	0.54	8		Low	AW
4	Lt VA	10	99.8	74.2	87.23		Normal	AW
		11	99.7	0.64	6.38		Low	AW
5	Lt ICA	12	99.9	0.48	98	Yes	Low	AW
		13	99.7	70.97	50		High	TW
6	Acom	14	99.9	64.51	87.5		Normal	Normal
		15	99.8	29.03	70.83		Low	TW
7	Rt MCA	16	100	0.95	80	Yes	Low	AW
		17	99.9	2.38	10		Low	Normal
8	Lt MCA	18	99.9	1.42	80	Yes	Low	AW
		19	99.9	1.42	10		Low	TW
9	Lt ICPC	20	100	2.85	92.59	Yes	Low	AW
		21	99.8	85.71	59.26		Normal	Normal
10	A2-A3	22	100	100	91.67		High	Normal
		23	99.9	25	12.5		Low	AW
11	Acom	24	100	0.41	91.67	Yes	Low	AW
		25	99.9	0.4	41.67		Low	AW
		26	100	0.2	66.67	Yes	Low	TW
12	Lt MCA	27	99.9	52	30		Normal	Normal
		28	99.7	0.2	66.67	Yes	Low	TW
13	Rt IC A2	29	99.6	52	33.33		Normal	Normal
		30	99.8	0.28	75	Yes	Low	AW
14	Lt MCA	31	99.4	0.28	33.33		Low	AW
		32	100	0.38	90.48	Yes	Low	TW
15	Acom	33	99.9	0.38	47.62		Low	normal
		34	99.8	342	75		High	TW
16	Rt MCA	35	100	0.71	85	Yes	Low	AW
		36	100	0.33	96.67	Yes	Low	AW
17	Lt ICPC	37	99.9	100	90		High	TW
		38	99.9	0.33	33.33		Low	TW
17	Lt ICPC	39	99.9	1	33.33		Low	TW

nP: normalized pressure, *nWSS*: normalized wall shear stress, *nVel*: normalized velocity, *hP*: high pressure, *IWSS*: low wall shear stress, *dWSSv*: divergent wall shear stress vectors, *hitSL*: hitting streamlines, *WSS*: wall shear stress, *Intraop*: intraoperative, *TW*: thin wall, *AW*: atherosclerotic wall

$0.8 \pm 0.8\%$ (range 0.3–2.9%), and the mean P was 99.9% compared to the parent vessel P (range 99.8–100%). The mean SL velocity was 84.5% compared to the parent vessel. Compared to aneurysm dome areas with normal appearance, normalized P , SL velocity and normalized SL velocity were significantly higher (p values 0.04, 0.02, and 0.004, respectively), whereas WSS, and normalized WSS were significantly lower (p values 0.0007 and 0.0002, respectively). In the other cases (20%) this association of parameters matched with TW areas (Fig. 2).

In TW areas, we identified low WSS (normalized WSS $4.6 \pm 9.9\%$, range 0.2–29%) in the majority of cases (75%), along with high P (mean $99.9 \pm 0.1\%$ compared to parent vessel P , range 99.7–100%), and low streamline velocity (mean $48 \pm 30\%$ compared to parent vessel SL velocity, range 8–90.5%) (Fig. 3). WSS and normalized WSS were significantly lower than aneurysm dome areas with normal appearance ($p = 0.006$ and 0.003, respectively). We also found that, in the majority of cases, TW areas are characterized by parallel WSS vectors (75%) and curved streamlines (75%).

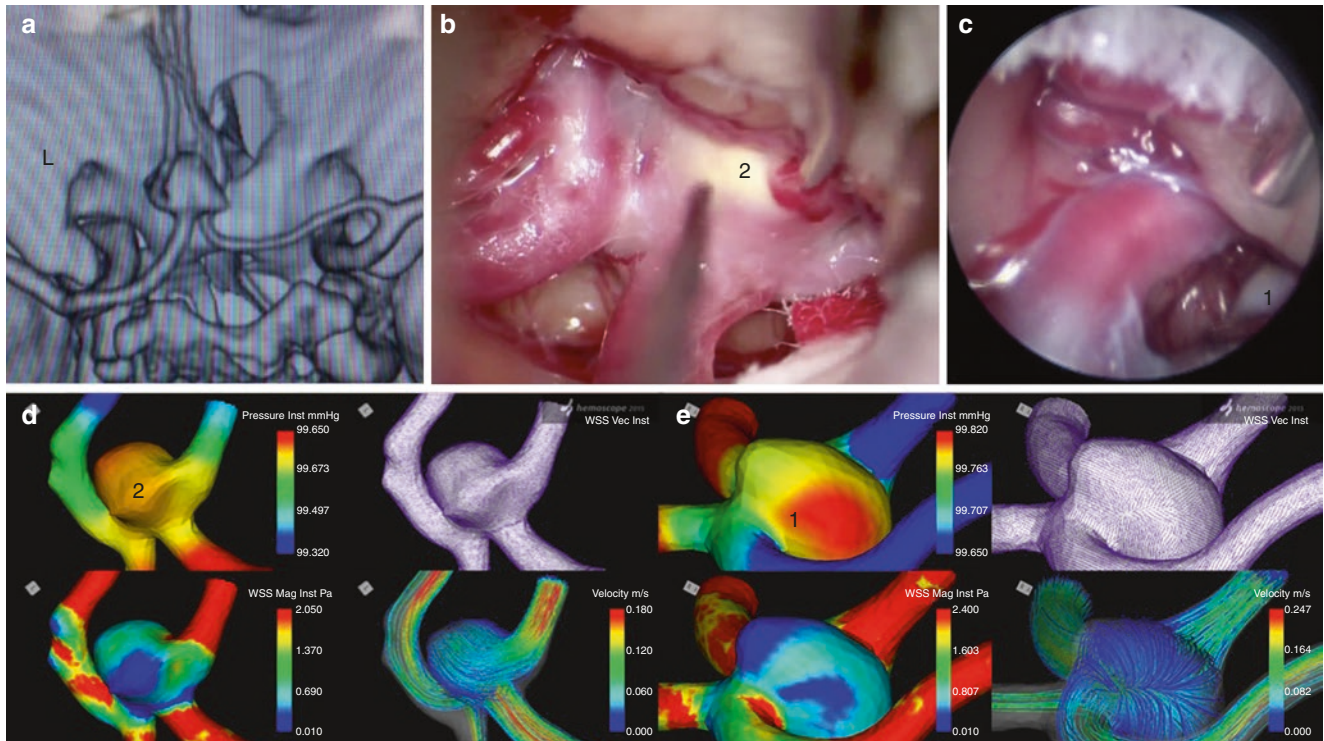


Fig. 1 Patient n.11. (a) 3D CT-scan reconstruction of the Acom aneurysm. (b) Intraoperative inspection demonstrating a yellowish and thick area (2). (c) Intraoperative endoscopic inspection revealing a second yellowish and thick area (1). (d, e) CFD analysis showing different

characteristics of the areas 1 and 2. In particular, area 1 reveals high P , low WSS, divergent WSS vectors, *streamlines* hitting the wall of the aneurysm with high velocity

Fig. 2 Patient n.14. (a) 3D CT-scan reconstruction of the left MCA aneurysm. (b) Intraoperative direct visualization revealed a TW bleb (1), in contrast with a normal wall dome (2). (c) CFD analysis showed the TW bleb to have high P , low WSS, divergent WSS vectors, and SL hitting the bleb wall with high velocity

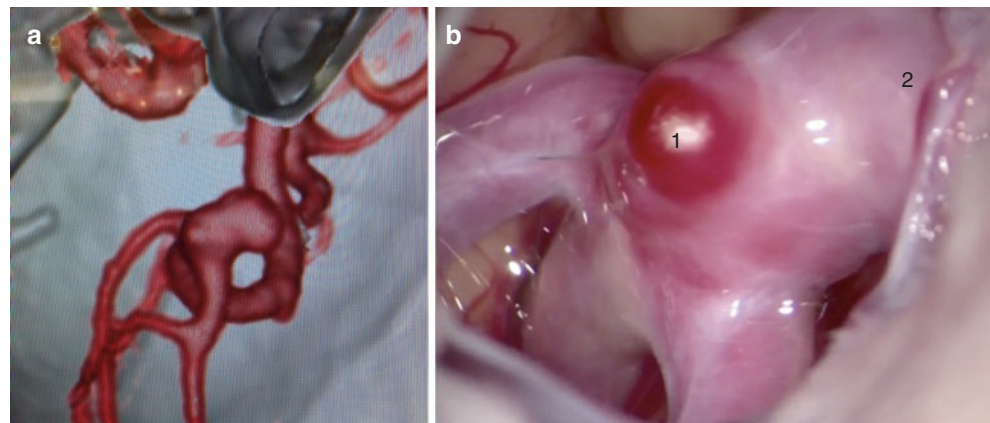


Fig. 2 (continued)

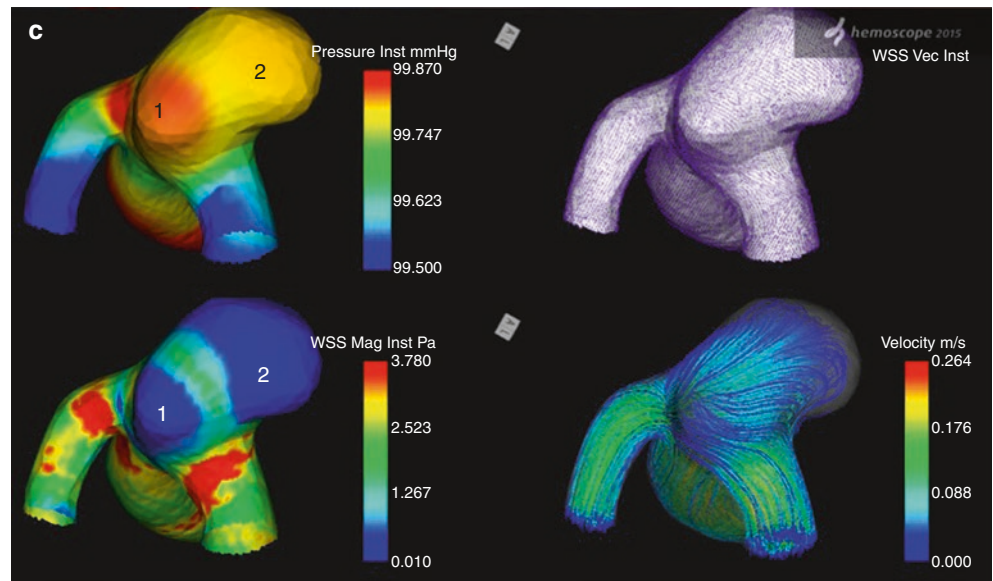
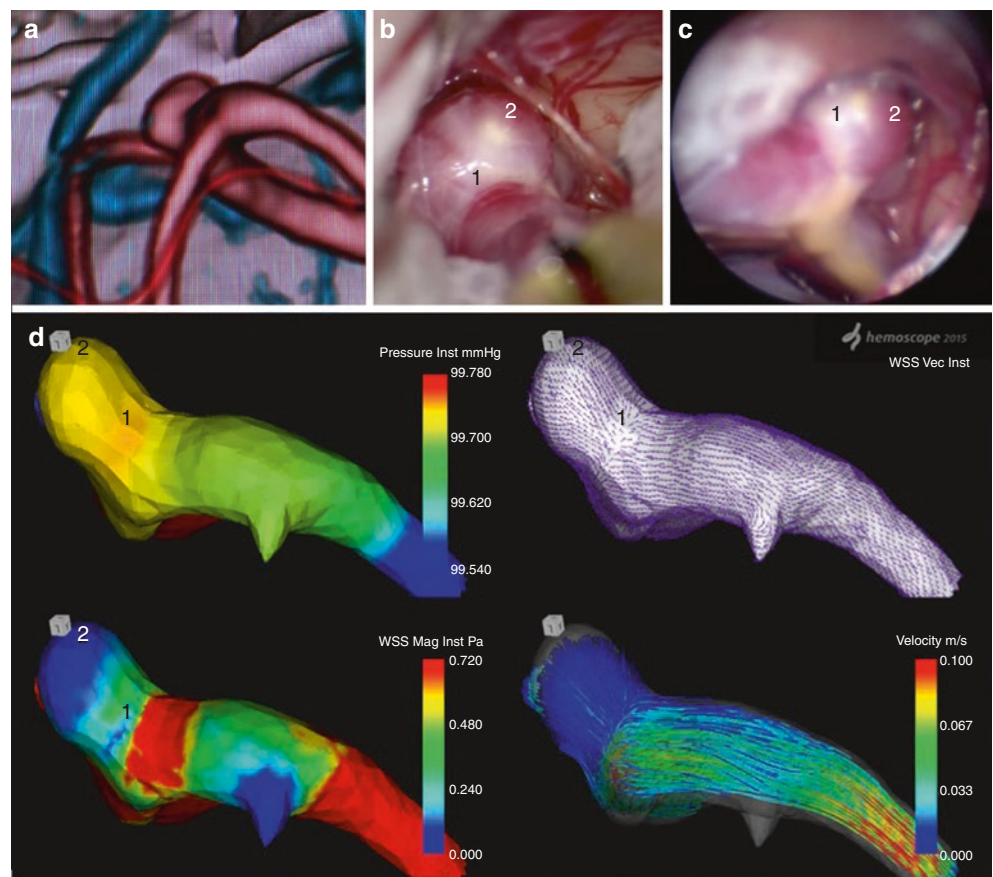


Fig. 3 Patient n.8. (a) 3D CT-reconstruction of left MCA aneurysm. (b, c) Intraoperative microscopic and endoscopic inspection revealing an AW area close to the neck of the aneurysm and a TW area at the tip of the dome. (d) CFD analysis showing the AW area with high P , low WSS, divergent vectors, and SL hitting with high velocity. The TW area has low WSS



Discussion

Computational fluid dynamics is a tool that allows the analysis of fluids through pipes and tube dilations. It has been applied to the study of intracranial vessels and aneurysms for

more than 15 years, and is regarded as a promising instrument to predict the natural history of aneurysms. However, conflicting results have been published about the interpretation of CFD parameters. Two theories explaining the mechanisms of cerebral aneurysm rupture have been proposed. Some authors reported that ruptured aneurysms have higher

WSS compared with unruptured aneurysms, although others stated that ruptured aneurysms have a lower WSS and higher OSI [4, 8]. More recently, Takao et al. showed that a low WSS may be associated with aneurysm rupture, but statistical significance was noted only in ICA cases and not in MCA cases [10]. The same study also investigated pressure loss coefficient (PLc), which represents the pressure loss associated with the shape of pipes and obstacles to flow. Interestingly, they showed that high PLc is associated with a higher risk of aneurysm rupture. This might be consistent with our findings of high P in the areas of thicker walls. Miura published similar results showing that low WSS is associated with rupture of MCA aneurysms [6]. Fukazawa et al. applied CFD to 12 ruptured MCA aneurysms, showing an association between the rupture point seen during operation and low WSS, lower-velocity areas, and complex flow patterns [11]. Similarly, Omodaka et al. found that the time-averaged WSS at the rupture point of six ruptured MCA aneurysms was significantly lower than that at the aneurysm wall without the rupture point [7]. Also Lu et al. associated low WSS with higher risk of rupture [5]. Bleb formation seems, however, to be associated with high WSS, which later falls after the formation of the bleb [2, 3]. More recently, a unifying theory has been proposed, hypothesizing that both high and low WSS could drive intracranial aneurysms growth and rupture. Mural cell-mediated (high WSS) and inflammatory cell-mediated (low WSS) destructive remodeling pathways have been involved in this process [12, 13].

The possible correlation between CFD results and the risk of aneurysm rupture is very intriguing, as it could be of great importance to stratify rupture risk and tailor treatment accordingly. However, CFD parameters related to blood flow and wall stress can be of great importance, even irrespective of aneurysm eventual rupture. Actually, the potential ability of CFD to provide information about the structural characteristics of the aneurysm wall can be a valuable tool during surgical dissection or coiling. All the available current imaging techniques can show the morphology and the anatomical relationships of the vessels and the aneurysm with adjacent structures, but nothing can be used to detect the thickness of the aneurysm wall. Although the majority of studies on CFD focused on the risk of rupture, fewer publications are available about the correlation between CFD parameters and the characteristics of the aneurysm wall. Kadasi et al. first reported the colocalization of TWRs with areas of low WSS and focal pressure elevation [1]. Suzuki et al. recently published a paper where they assessed 50 aneurysm wall surfaces and investigated the correlation between pressure elevation and TWRs [9]. They found that most P_{\max} areas (82%) corresponded with TWRs.

Our study also found a co-localization of low WSS and TWRs. However, low WSS can also be found in areas of the aneurysm dome that are not thin and red. Moreover, in some

cases, red, thin walls do not show a low WSS (30% of cases in our series). We also noticed that when low WSS is associated with high pressure, divergent WSS vectors, and streamlines hitting the wall with high velocity, the surface is more likely thick, yellow, and atherosclerotic (78.6% of cases in our series).

We hypothesize that continuous high velocity blood flow hitting an area of the aneurysm could trigger a remodeling of the wall, ultimately leading to a reactive thickening. In this perspective, areas with low WSS but stagnating blood flow can be more prone to thinning remodeling as a consequence of an inflammatory process, as already described in other studies. We also think that, at this stage, CFD analysis can provide only a general but intriguing picture of the association between fluid dynamics parameters and intraoperative findings. This can be caused by many reasons. First, aneurysm initiation, growth, and eventual rupture are long and complex processes. By definition, aneurysm architecture often changes over time, and fluid dynamics in the aneurysm are likely to change accordingly. CFD analysis is a representation of the aneurysm fluid dynamics at a specific time point, and it is therefore very difficult to foresee the natural evolution of the aneurysm from a single static picture. CFD data from a very large population of patients could maybe provide a wider representation of different aneurysm stages at different locations, and finally help clinicians to refine the ability to predict the natural history of the disease. Another reason for the difficulty in providing a unique and comprehensive interpretation of CFD results is the fact that other factors different from fluid dynamics can influence aneurysm evolution, for example, genetics, and the environment around the aneurysm itself. Moreover, the currently available software, although advanced, might still be limited to provide a fully detailed analysis of the multiple variables playing a role in the fluid dynamics in vivo.

Our study is therefore affected by limitations that are common to previously published papers about CFD analysis. These limitations depend on the pre-processing assumptions of Newtonian fluid models with fixed density and viscosity, vessel rigidity. Moreover, we did not consider aneurysm histology, peri-aneurysm anatomy, or humoral and physiological parameters. The AW and TW areas evaluation method was subjective and based only on visual intraoperative findings. The boundary conditions were uniform across all cases, although patient-specific analysis requires boundary conditions established with magnetic resonance imaging and echocardiographic imaging.

Despite the current limitations of CFD analysis applied to clinical settings, and the limited number of patients, our results show that red, thin areas on aneurysm walls often have a low WSS, consistent with previously published papers. Therefore, attention must be taken when approaching areas with a low WSS. Moreover, we noticed that the asso-

ciation of high pressure, low WSS, divergent WSS vectors, and SL hitting the wall with high velocity is most often associated with thickening of the aneurysm wall.

Conflict of Interest The authors declare that they have no conflict of interest.

References

1. Kadasi LM, Dent WC, Malek AM. Colocalization of thin-walled dome regions with low hemodynamic wall shear stress in unruptured cerebral aneurysms. *J Neurosurg.* 2013;119:172–9.
2. Russell JH, Kelson N, Barry M, Percy M, Fletcher DF, Winter CD. Computational fluid dynamic analysis of intracranial aneurysmal bleb formation. *Neurosurgery.* 2013;73:1061–8.
3. Cebal JR, Castro MA, Burgess JE, Pergolizzi RS, Sheridan MJ, Putman CM. Characterization of cerebral aneurysms for assessing risk of rupture by using patient-specific computational hemodynamics models. *AJNR Am J Neuroradiol.* 2005;26:2550–9.
4. Cebal JR, Mut F, Weir J, Putman C. Quantitative characterization of the hemodynamic environment in ruptured and unruptured brain aneurysms. *AJNR Am J Neuroradiol.* 2011;32:145–51.
5. Lu G, Huang L, Zhang XL, Wang SZ, Hong Y, Hu Z, Geng DY. Influence of hemodynamic factors on rupture of intracranial aneurysms: patient-specific 3D mirror aneurysms model computational fluid dynamics simulation. *AJNR Am J Neuroradiol.* 2011;32:1255–61.
6. Miura Y, Ishida F, Umeda Y, Tanemura H, Suzuki H, Matsushima S, Shimosaka S, Taki W. Low wall shear stress is independently associated with the rupture status of middle cerebral artery aneurysms. *Stroke.* 2013;44:519–21.
7. Omodaka S, Sugiyama S, Inoue T, Funamoto K, Fujimura M, Shimizu H, Hayase T, Takahashi A, Tominaga T. Local hemodynamics at the rupture point of cerebral aneurysms determined by computational fluid dynamics analysis. *Cerebrovasc Dis.* 2012;34:121–9.
8. Xiang J, Natarajan SK, Tremmel M, Ma D, Mocco J, Hopkins LN, Siddiqui AH, Levy EI, Meng H. Hemodynamic-morphologic discriminants for intracranial aneurysm rupture. *Stroke.* 2011;42:144–52.
9. Suzuki T, Takao H, Suzuki T, Kambayashi Y, Watanabe M, Sakamoto H, Kan I, Nishimura K, Kaku S, Ishibashi T, Ikeuchi S, Yamamoto M, Fujii Y, Murayama Y. Determining the presence of thin-walled regions at high-pressure areas in unruptured cerebral aneurysms by using computational fluid dynamics. *Neurosurgery.* 2016;79:589–95.
10. Takao H, Murayama Y, Otsuka S, Qian Y, Mohamed A, Masuda S, Yamamoto M, Abe T. Hemodynamic differences between unruptured and ruptured intracranial aneurysms during observation. *Stroke.* 2012;43:1436–9.
11. Fukazawa K, Ishida F, Umeda Y, Miura Y, Shimosaka S, Matsushima S, Taki W, Suzuki H. Using computational fluid dynamics analysis to characterize local hemodynamic features of middle cerebral artery aneurysm rupture points. *World Neurosurg.* 2015;83:80–6.
12. Meng H, Tutino VM, Xiang J, Siddiqui A. High WSS or low WSS? Complex interactions of hemodynamics with intracranial aneurysm initiation, growth, and rupture: toward a unifying hypothesis. *AJNR Am J Neuroradiol.* 2014;35:1254–62.
13. Xiang J, Tutino VM, Snyder KV, Meng H. CFD: computational fluid dynamics or confounding factor dissemination? The role of hemodynamics in intracranial aneurysm rupture risk assessment. *AJNR Am J Neuroradiol.* 2014;35:1849–57.